EPR Spectroscopy

Anisotropic Hyperfine Interaction in the Manganese(III) Hexaaqua Ion

Itana Krivokapič, Chris Noble, Søren Klitgaard, Philip Tregenna-Piggott, Høgni Weihe,* and Anne-Laure Barra*

The manganese(III) ion is ubiquitous among chemical systems that exhibit intriguing biological and physical properties, ranging from photosystem II and superoxide dismutase to the celebrated single-molecule magnet Mn_{12}. It is for this reason that complexes and clusters of the manganese(III) ion are widely recognized as the delicicae of high-field electron paramagnetic resonance (EPR) spectroscopists,[1] the fact that they invariably yield good-quality spectra being but a secondary consideration.[2–7]

Hitherto, the spatial property of the hyperfine interaction between the $S = 2$ electronic spin and the $I = 5/2$ nuclear spin in any chemically relevant manganese(III) compound has escaped observation. There are two fundamental reasons why knowledge of the hyperfine interaction energies is important. First, the magnitude and sign of the anisotropy relate directly to the manganese(III) coordination sphere. Secondly, the hyperfine interaction has been demonstrated to be instrumental in quantum tunneling of the magnetization in single-molecule magnets.[8,9]

In an EPR study of manganese(III) superoxide dismutase,[2] the hyperfine splittings were resolved and compared to those documented for a photo-oxidation product of manganese(III) in the high-affinity site of photosystem II. Consistency was found between the observed hyperfine splitting and the sign of the zero-field-splitting parameter in the two systems. However, these experiments were confined to X-band parallel-mode experiments, which can determine just one component of the hyperfine interaction matrix. Information concerning the spatial property of the hyperfine interaction matrix requires the use of higher frequencies, as shown in a study of manganese(III)-doped rutile.[12]

In this communication we report single-crystal and powder EPR spectra of the $[Mn(H_2O)_6]^{3+}$ ion at high fields and multiple frequencies. To minimize line broadening due to spin–spin dipolar interactions, the $[Mn(H_2O)_6]^{3+}$ ion was doped into the diamagnetic cesium gallium alum, $Cs[Ga(H_2O)_6](SO_4)_2 \cdot 6H_2O$, thus enabling the precise determination of the metal hyperfine interaction parameters.

Pale orange–red crystals of this sample were grown at 0 °C from a saturated 6 M sulfuric acid solution of the cesium gallium alum that contained 1 % cesium manganese alum. A trace of the corresponding chromium(III) alum was also added. The EPR lines of $[Cr(OH_2)_6]^{3+}$ were readily identified and were useful for crystal alignment.

The single-crystal EPR spectra exhibited several magnetically nonequivalent species, reflecting the space group of the host and the propensity of the $[Mn(OH_2)_6]^{3+}$ ion to distort along a Jahn–Teller active coordinate. There are four tervalent cations in the cubic unit cell, each occupying a site of S_6 symmetry on one of the four unique threefold axes of the unit cell. In addition, at low temperatures the $[Mn(OH_2)_6]^{3+}$ ion is expected to be locked into one of the three possible tetragonally elongated structures that results from the Jahn–Teller interaction. Such a distortion is clearly identified in the neat cesium manganese alum, which undergoes a phase transition from cubic to orthorhombic at 156 K. In the low-temperature phase, the metal ion is situated on a site with point symmetry C_i.[14] A total of twelve magnetically nonequivalent species is therefore anticipated for cesium gallium alum doped with manganese(III) ions, and the principal axes of the various interaction tensors are expected to be aligned close to the Mn–O bonds. Since the vectors of the Mn–O bonds are very closely aligned with the pseudo-crystallographic fourfold axes of the cubic unit cell, the

[*] I. Krivokapič, Dr. C. Noble, Priv.-Doz. Dr. P. Tregenna-Piggott
Laboratory for Neutron Scattering
ETH Zürich and Paul Scherrer Institute
5232 Villigen PSI (Switzerland)
Fax: (+41) 56-310-2939
E-mail: philip.tregenna@psi.ch
S. Klitgaard, Dr. H. Weihe
Department of Chemistry
University of Copenhagen
Universitetsparken 5, 2100 Copenhagen (Denmark)
E-mail: weihe@kiku.dk
Dr. A.-L. Barra
LCMI-CNRS B.P. 166
38042 Grenoble cedex 9 (France)

 DOI: 10.1002/ange.200463084

spectra are expected to simplify when the external magnetic field is aligned along one of these axes.

This expectation is, indeed, found to be the case. Figure 1 shows a 190-GHz spectrum taken between 0 and 6 T and obtained with the magnetic field parallel to a crystallographic

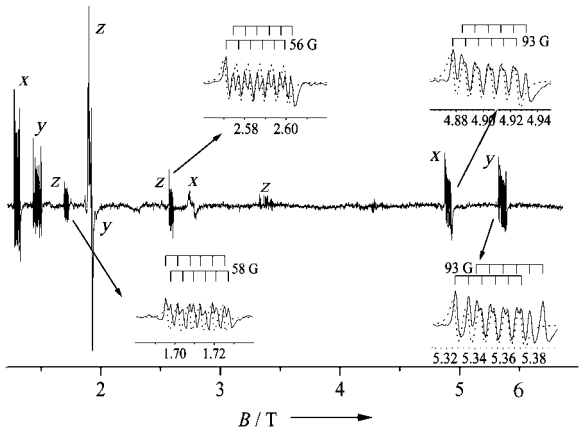

Figure 1. Single-crystal 190-GHz spectrum of the manganese(III) ion in cesium gallium alum obtained at 5 K with the magnetic field vector parallel to a crystallographic fourfold axis. Transitions corresponding to the magnetic field that is parallel to the molecular *x*, *y*, or *z* axis are designated accordingly. The inserts show the spacing between the hyperfine components of the least-complicated features in the spectrum. The simulated[10] spectra (dotted lines in the inserts) were calculated with the spin Hamiltonian parameters given in Equation (3).

fourfold axis. The spectrum exhibits several electronic transitions, each being split into a sextet due to the hyperfine interaction. Two types of sextets are identified in the spectrum: one in which the separation between neighboring lines is 92–93 Gauss; the other in which this splitting is 56–58 Gauss. Each electronic transition is doubled but this doubling is not found in the powder spectra, representative examples of which are shown in Figure 2. Therefore, the doubling must be due to either crystal twinning, a small misalignment when orienting the crystal, or a result of magnetically nonequivalent $[Mn(OH_2)_6]^{3+}$ ions that differ in terms of the orientation of the threefold axes for the sites on which they lie. Rotation of the magnetic field less than 10° away from the fourfold axis has the effect of rendering all sites magnetically nonequivalent, and the complexity of the spectrum increases enormously. The smaller hyperfine splitting of 57 Gauss appears again in the parallel-mode X-band spectra shown in Figure 3. The overlap of lines arising from magnetically nonequivalent species can be seen clearly, as the crystal is rotated in the {110} plane, away from the fourfold axis.

The hyperfine lines in the single-crystal spectra in Figures 1 and 3 were interpreted in terms of a spin Hamiltonian for $(S,I) = (2, 5/2)$.[11] In Equation (1), the five first terms describe the zero-field splittings, and the remaining lines describe the Zeeman energy and the hyperfine interaction.

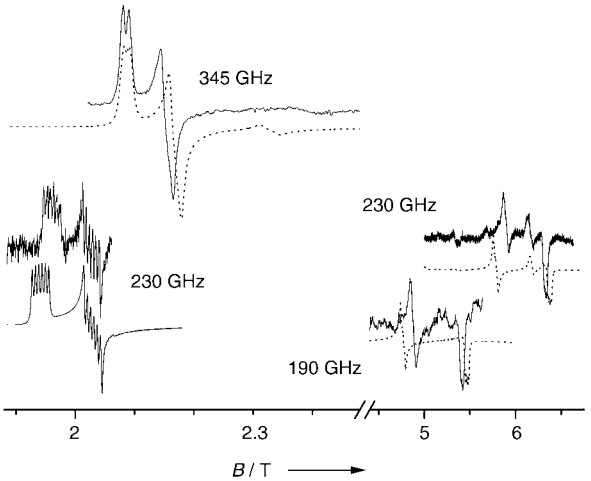

Figure 2. The strongest features (upper traces) in the EPR spectra of a powdered sample of the manganese(III) hexaaqua ion in cesium gallium alum. The frequencies used are designated. Only the field ranges 1.9–2.5 T and 4.5–6.7 T are shown. The separation between the hyperfine components of the low-field 230-GHz spectrum is 93 ± 1 Gauss. The simulated spectra (lower traces) are calculated with the parameters obtained from the single-crystal spectra [Eq. (3)]. All simulated spectra are obtained by using the same bandwidth (70 G) for each hyperfine line.

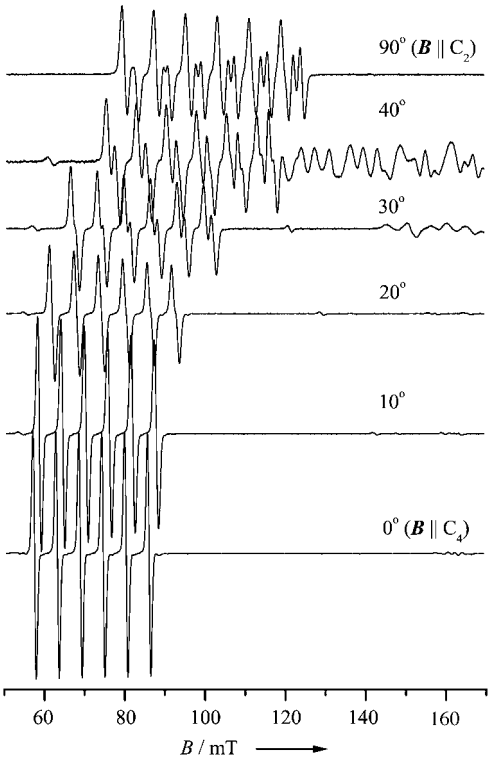

Figure 3. Single-crystal parallel-mode X-band spectra recorded with the magnetic field in the (110) crystallographic plane. The frequencies varied between 9.3107 and 9.3114 GHz. The angle indicated for each spectrum designates the angle between the crystallographic fourfold axis and the vector of the magnetic field. The separation between the hyperfine components in the low-field portion of the six spectra is 57, 58, 61, 66, 75, and 80 Gauss going from the bottom trace to the top.

$$\begin{aligned}\hat{\mathscr{H}} =& D(\hat{S}_z^2-2) + E(\hat{S}_x^2-\hat{S}_y^2)\\ &+B_4^4\frac{1}{2}[\hat{S}_+^4+\hat{S}_-^4] + B_0^4[35\hat{S}_z^4-155\hat{S}_z^2+72]\\ &+B_2^4\frac{1}{4}[(7\hat{S}_z^2\text{-}11)(\hat{S}_+^2+\hat{S}_-^2)+(\hat{S}_+^2+\hat{S}_-^2)(7\hat{S}_z^2-11)]\\ &+\mu_B(g_x B_x \hat{S}_x + g_y B_y \hat{S}_y + g_z B_z \hat{S}_z)\\ &+A_x \hat{S}_x \hat{I}_x + A_y \hat{S}_y \hat{I}_y + A_z \hat{S}_z \hat{I}_z\end{aligned} \quad (1)$$

The lines in the spectrum of Figure 1 as well as the low-angle lines in Figure 3 were assigned to specific transitions of this spin system, and the spin Hamiltonian parameters of Equation (1) were obtained by minimizing χ^2 in Equation (2). N is the number of observations; $B_{i,\mathrm{obs}}$ and $B_{i,\mathrm{calc}}$ are the observed and calculated ith resonance magnetic field, respectively. σ_i is an uncertainty associated with the ith observation and was set to a fraction of the bandwidth for most of the observations.

$$\chi^2 = \sum_{i=1}^{N} \frac{(B_{i,\mathrm{obs}}-B_{i,\mathrm{calc}})^2}{\sigma_i^2} \quad (2)$$

By using a total of 84 resonance magnetic fields in the fit and setting $g_x = g_y$ as well as $A_x = A_y$ as directly suggested by the experimental data (Figure 1), we were able to obtain the parameter values listed in Equation (3).

$$\begin{aligned}D &= -4.514(1)\ \mathrm{cm}^{-1}\\ E &= -0.161(5)\ \mathrm{cm}^{-1}\\ B_0^4 &= -0.0041(5)\ \mathrm{cm}^{-1}\\ B_2^4 &= -0.00014(5)\ \mathrm{cm}^{-1}\\ B_4^4 &= -0.00577(7)\ \mathrm{cm}^{-1}\\ g_x &= g_y = 2.000(1)\\ g_z &= 1.9844(6)\\ A_x &= A_y = -0.0087(2)\ \mathrm{cm}^{-1}\\ A_z &= -0.00531(5)\ \mathrm{cm}^{-1}\end{aligned} \quad (3)$$

These parameter values were then used to reproduce the powder spectra in Figure 2. The agreement is certainly acceptable. In reference [3] values for D and $|E|$ of $-4.491(7)\ \mathrm{cm}^{-1}$ and $0.248\ \mathrm{cm}^{-1}$, respectively, were derived from an EPR study of $Cs[Mn(OD_2)_6](SO_4)_2\cdot 6H_2O$, with a small but significant change in these parameters noted upon hydrogen-for-deuterium isotopic substitution. Note that the value of the orthorhombic zero-field splitting parameter E is slightly larger in magnitude than that determined for the diluted alum in the present study. The discrepancy is primarily a result of the large linewidths obtained for the undiluted alum, which made an inclusion of the fourth-order zero-field splitting parameters unwarranted. The parameters E and B_4^4 are somewhat negatively correlated, and a precise definition requires data from a range of frequencies, including X-band measurements, which are tractable only if the EPR linewidths are sufficiently narrow. The similar values of D suggests that the structure and bonding in the $[Mn(OD_2)_6]^{3+}$ is similar in the two systems.

With the choice of $E<0$ we see that the fourth-order spin Hamiltonian parameters B_0^4, B_2^4, and B_4^4 are all found to be negative, which was also found to be the case for $[Mn(cyclam)Br_2]Br$.[6] (cyclam = 1,4,8,11-tetraazacyclotetradecane). An analysis of this result, however, is not relevant in the present context and will not be discussed here.

The g values, with $g_x, g_y > g_z$, conform to what is expected for an elongated coordination sphere. According to a previous report, the relation $g_x - g_z = 2\zeta/3\Delta_{T_2}$ holds.[15] In this equation, ζ is the spin–orbit coupling parameter, and Δ_{T_2} is the energy separation between the ground-spin quintet and the $^5T_2$ (O notation) excited term. Using the experimentally determined $\Delta_{T_2} = 21\,400\ \mathrm{cm}^{-1}$[3] we find $\zeta = 223\ \mathrm{cm}^{-1}$, which corresponds to 63% of the free-ion value. In Equation (3), we have explicitly set the values of the hyperfine splitting constants as negative. The fit cannot discriminate between the possible sign combinations of these parameters. However, based on other arguments, presented below, we conclude that the parameters are negative.

The angular variation of the resonance magnetic fields as well as the angular variation of the separation between the hyperfine splitting components in Figure 3 is very well described by the effective spin Hamiltonian with $S=\frac{1}{2}$ for a non-Kramers doublet involving only the $+2$ and -2 M_S components in Equation (4), in which θ is the angle between the magnetic field vector and the elongation axis of the coordination sphere.

$$\hat{\mathscr{H}}_{\mathrm{approx}} = b\hat{S}_x + \mu_B g_z' \hat{S}_z B\cos\theta + A_z' \hat{S}_z \hat{I}_z \quad (4)$$

The parameters b, g_z', and A_z' of this effective Hamiltonian are related to those of Equation (1). It can be shown that to the second order in the perturbation theory, the zero-field splitting b of the two components is given by Equation (5).

$$b = 24B_4^4 + \frac{(\sqrt{6}E+\sqrt{54}B_2^4)^2}{2D-30B_0^4} \quad (5)$$

With the parameter values determined above, we see that the first and second term on the right-hand side of the equation have the same sign and are comparable in magnitude. The effective g_z' factor and the effective hyperfine splitting constant A_z' are related to g_z and A_z by Equations (6) and (7).

$$g_z' = 4g_z \quad (6)$$

$$A_z' = 4A_z \quad (7)$$

The effective Hamiltonian Equation (4) is applicable when the $|\pm 2\rangle$ components are well isolated from the remaining components of the spin quintet and when $h\nu > b$, ν being the spectrometer frequency, which is the case here. Using Equation (4) to interpret the spectra in Figure 3 only confirms Equations (6) and (7) and gives $|b| = 0.172\ \mathrm{cm}^{-1}$, which is in reasonable agreement with the value calculated from the formula for the second-order perturbation theory, Equation (5), $b = -0.156\ \mathrm{cm}^{-1}$. With the Hamiltonian Equation (4) the separation between neighboring hyperfine lines is,

to a good approximation, given by Equation (8).

$$B_r(M_I)-B_r(M_I-1) \approx \frac{A'_z}{g'_z \mu_B \cos\theta} \quad (8)$$

The experimental hyperfine line separations of the spectra in Figure 3 are reproduced within 1 Gauss by Equation (8).

For the tetragonally elongated coordination sphere, the relations in Equations (9) and (10) can be derived for the hyperfine coupling constants.[2,15]

$$A_z = P\left(\frac{1}{7}-\kappa-\frac{2\zeta}{\Delta_{T_2}}\right) = P\left(\frac{1}{7}-\kappa+(g_z-2.0023)\right) \quad (9)$$

$$A_x = A_y = P\left(-\frac{1}{14}-\kappa-\frac{\zeta}{2\Delta_{T_2}}\right) = P\left(-\frac{1}{14}-\kappa+(g_x-2.0023)\right) \quad (10)$$

The parameter κ for manganese(III) has been determined to be approximately 0.5.[12] Hence the term in parentheses becomes negative and we conclude that both hyperfine coupling constants are negative because the parameter P for ^{55}Mn is positive. Using Equations (9) and (10) together with the experimentally determined A values and the deviation of the g values from the free-electron g value, we obtain $P = 0.0170\ cm^{-1}$ and $\kappa = 0.43$. P depends on the expectation value $\langle r^{-3}\rangle$, as does the spin–orbit coupling parameter ζ; therefore, it can be expected to be related to the free-ion value in a similar way as the spin–orbit coupling parameter is related to the free-ion value. This is indeed the case; the free-ion value of P for manganese(III) has been calculated to $0.0212\ cm^{-1}$, and our value for the manganese(III) hexaaqua ion corresponds to 80% of this free-ion value, which is in good agreement with the spin–orbit coupling reduction (see above). In comparison, for rutile: Mn^{3+} $P = 0.0140\ cm^{-1}$. The average metal–oxygen bond length in rutile and $[Mn(H_2O)_6]^{3+}$ is 1.956 Å and 1.994 Å, respectively.[13,14] As shorter bond lengths are associated with stronger overlaps between metal- and oxygen-centered orbitals it is also expected that $P(\text{rutile}) < P([Mn(H_2O)_6]^{3+})$. By the same token, P is expected to be further reduced for a metal center that is surrounded by donors softer than oxygen.

In summary, we have presented the first observation and interpretation of the anisotropic hyperfine interaction in a chemically relevant monomeric complex that contains the manganese(III) ion. The hyperfine interaction parameters are related to more fundamental parameters such as the spin–orbit coupling parameter, as well as excited-state energies obtained from the absorption spectrum, which has been analyzed in detail. Basically, the analyses performed here are based on ligand–field theory, which offers a consistent description of the situation. A comprehensive treatment requires that Jahn–Teller coupling be considered explicitly, as dynamic effects can have profound effect on all the orbital electronic operators. This will be the topic of a paper currently in preparation.

Received: December 28, 2004
Published online: May 2, 2005

Keywords: EPR spectroscopy · hyperfine interactions · magnetic properties · manganese

[1] A.-L. Barra, D. Gatteschi, R. Sessoli, G. L. Abbati, A. Cornia, A. C. Fabretti, M. G. Uytterhoeven, *Angew. Chem.* **1997**, *109*, 2423 – 2426; *Angew. Chem. Int. Ed. Engl.* **1997**, *36*, 2329 – 2331.
[2] K. A. Campbell, D. A. Force, P. J. Nixon, F. Dole, B. A. Diner, D. R. Britt, *J. Am. Chem. Soc.* **2000**, *122*, 3754 – 3761.
[3] P. L. W. Tregenna-Piggott, H. Weihe, A.-L. Barra, *Inorg. Chem.* **2003**, *42*, 8504 – 8508.
[4] J. Krzystek, J. Telser, L. A. Pardi, D. P. Goldberg, B. M. Hoffman, L.-C. Brunel, *Inorg. Chem.* **1999**, *38*, 6121 – 6129.
[5] S. Mossin, H. Weihe, A.-L. Barra, *J. Am. Chem. Soc.* **2002**, *124*, 8764 – 8765.
[6] S. Mossin, M. Stefan, P. ter Heerdt, A. Bouwen, E. Goovaerts, H. Weihe, *Appl. Magn. Reson.* **2001**, *21*, 578 – 596.
[7] R. Basler, P. L. W. Tregenna-Piggott, H.-P. Andres, C. Dobe, H.-U. Güdel, S. Janssen, G. J. McIntyre, *J. Am. Chem. Soc.* **2001**, *123*, 3377 – 3378.
[8] W. Wernsdorfer, R. Sessoli, D. Gatteschi, *Europhys. Lett.* **1999**, *47*, 254 – 259.
[9] W. Wernsdorfer, A. Caneschi, R. Sessoli, D. Gatteschi, A. Cornia, V. Villar, C. Paulsen, *Phys. Rev. Lett.* **2000**, *84*, 2965 – 2968.
[10] J. Glerup, H. Weihe, *Acta Chem. Scand.* **1991**, *45*, 444 – 448; C. J. H. Jacobsen, E. Pedersen, J. Villadsen, *Inorg. Chem.* **1993**, *32*, 1216 – 1221.
[11] A. Abragam, B. Bleaney, *Electron Paramagnetic Resonance of Transition Ions*, Oxford University Press, Oxford, **1970**.
[12] H. J. Gerritsen, E. S. Sabisky, *Phys. Rev.* **1963**, *132*, 1507 – 1512.
[13] A. F. Wells, *Structural Inorganic Chemistry*, Clarendon, Oxford, **1984**.
[14] P. L. W. Tregenna-Piggott, H. P. Andres, G. J. McIntyre, S. P. Best, C. C. Wilson, J. A. Cowan, *Inorg. Chem.* **2003**, *42*, 1350 – 1365.
[15] J. S. Griffith, *The Theory of Transition Metal Ions*, Cambridge University Press, Cambridge, **1961**.

